# Graphene Oxides Dispersing and Hosting Graphene Sheets for Unique Nanocomposite Materials

**Leilei Tian, Parambath Anilkumar, Li Cao, Chang Yi Kong,[†] Mohammed J. Meziani, Haijun Qian,[‡] L. Monica Veca, Tim J. Thorne, Kenneth N. Tackett, II, Travis Edwards, and Ya-Ping Sun***

Department of Chemistry and Laboratory for Emerging Materials and Technology, Clemson University, Clemson, South Carolina 29634-0973, United States [†] On leave from Department of Materials Science and Chemical Engineering, Faculty of Engineering, Shizuoka University, 3—5—1 Johoku, Naka-ku, Hamamatsu 432—8561, Japan [‡] Affiliated with Clemson University Electron Microscope Facility

**ABSTRACT** Graphene oxides (GOs), beyond their widely reported use as precursors for single-layer graphene sheets, are in fact excellent materials themselves (polymers in two-dimension, polyelectrolyte-like, aqueous solubility and biocompatibility, *etc.*). In this reported work we used aqueous GOs to effectively disperse few-layer graphene sheets (GNs) in suspension for facile wet-processing into nanocomposites of GNs embedded in GOs (as the polymeric matrix). The resulting lightweight and plastic-like nanocomposite materials remained mechanically flexible even at high loadings of GNs, and they were found to be highly efficient in thermal transport, with the experimentally determined thermal diffusivity competitive to those typically observed only in well-known thermally conductive metals such as aluminum and copper. As demonstrated, GOs apparently represent a unique class of two-dimensional polymeric materials for potentially "all-carbon" nanocomposites, among others, which may find technological applications independent of those widely proclaimed for graphene sheets.

**KEYWORDS:** graphene · graphene oxide · nanocomposite · thermal diffusivity · polymeric film

Graphene sheets, both single-layer and fewer-layer, have attracted much recent attention for their unique and/or superior properties, such as high mechanical strength, large carrier mobility and ballistic transport, and extreme thermal conductivity.[1−6] For the preparation of single-layer graphene in a popular wet chemical exfoliation route, graphite is exhaustively oxidized under harsh conditions to yield readily exfoliated graphene oxides (GOs or "G-Os" used recently in some literature to distinguish from the use of GOs as acronym specifically for graphite oxides), followed by their conversion back to graphene.[6] While the effectiveness or even feasibility is still in debate on the conversion of GOs to restore the intrinsic graphene structure,[6−10] there is an emerging recognition on the excellent properties of GOs themselves for material applications.[11−16] In particular, GOs are effectively polyelectrolytes, with a demonstrated ability in homogeneously dispersing carbon nanotubes to form relatively stable aqueous suspensions for subsequent device fabrication and other purposes.[17−19] Here we report that GOs are not only effective dispersion agents for other carbon nanomaterials but also unconventional polymeric matrices for nanocomposites. We used aqueous GOs to disperse graphene sheets (also referred to as platelets) in suspension for facile wet-processing into nanocomposites of graphene sheets embedded in the matrix of GOs. The nanocomposite films thus obtained remained mechanically flexible even at high loadings of graphene sheets. As an example of their superior properties, these lightweight plastic-like materials were found to be highly efficient in thermal transport, with experimentally determined thermal diffusivity values comparable with those in well-known thermally conductive metals such as aluminum and copper. The reported work serves to demonstrate the great potential of GOs as a unique class of two-dimensional polymeric materials, for potentially "all-carbon" nanocomposites, among others, which may find technological applications independent of those widely proclaimed for graphene sheets.

## RESULTS AND DISCUSSION

Fewer-layer graphene sheets (GNs, also referred to as GN platelets) were prepared by the exfoliation of a commercially supplied sample of expanded graphite with a combination of alcohol and oxidative acid treatments.[20] First, the graphite sample was stirred and vigorously sonicated in an alcohol—water mixture. Upon recovery, the sample was suspended in a precooled concentrated nitric—sulfuric acid and

* Address correspondence to syaping@clemson.edu.

Received for review January 15, 2011 and accepted March 15, 2011.

**Published online March 16, 2011**
**10.1021/nn200162z**

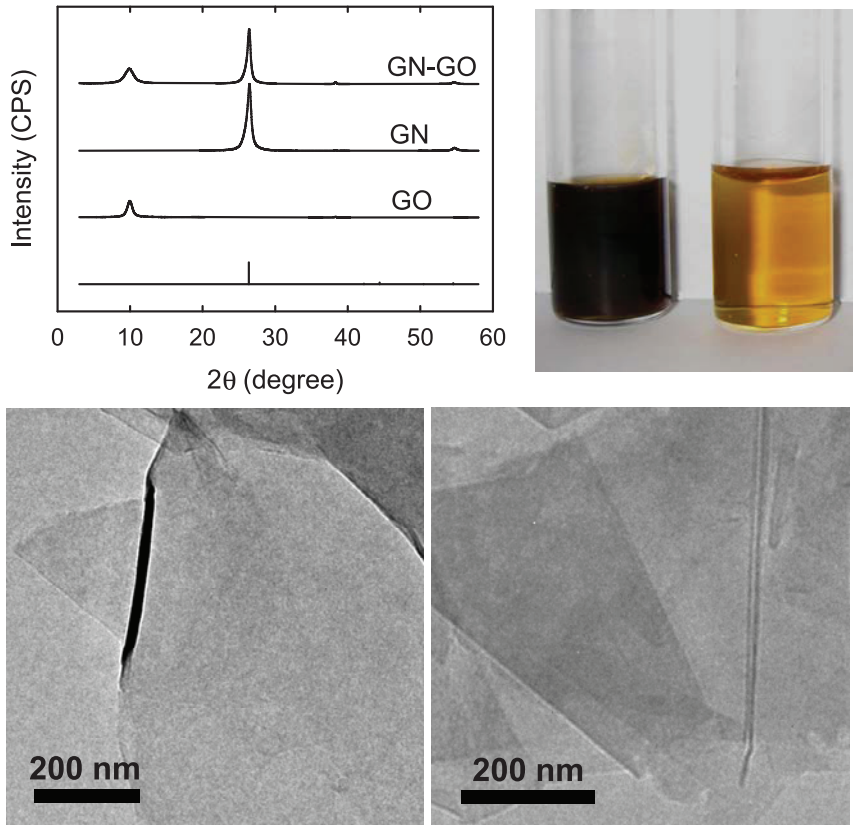


**Figure 1. Top-left: X-ray diffraction patterns of the samples as marked are compared with that of bulk graphite. Top-right: photos of aqueous solutions (left, concentrated; right, 1/10 diluted) of GOs from the Hummers method. Bottom: typical TEM images for specimens of GOs (left) and GNs (right).**

vigorously sonicated. The resulting GNs, despite the oxidative acid treatment, maintained graphitic structures, which were reflected in the X-ray diffraction results of the sample (Figure 1).

GOs of mostly single-layer sheets were prepared from the same commercial graphite sample by using the Hummers method with minor modification,[21] coupled with the subsequent exfoliation procedure already established in the literature.[11] The as-prepared GOs in the acid form (due to the oxidation of carbons at graphene sheet edges and defects into carboxylic acids) were converted to the salt form in base treatment, with the purpose of making their aqueous dispersion more stable (Figure 1).[11,19] Results from Raman spectroscopy characterization suggested no meaningful difference between the acid and salt forms of GOs, with the G-band and D-band features for both samples similar to those already reported in the literature.[22] The aqueous dispersion upon dilution was used to prepare specimens for TEM characterization. The images, in comparison with those of the GNs in Figure 1, suggest that the GOs were indeed mostly single sheets. No graphitic peak was found in X-ray diffraction results of the GOs (Figure 1), as expected from the conclusion in the literature that GOs prepared by the Hummers method and subsequent treatments are mostly single-layer sheets.

In the dispersion of GNs by GOs, a weighed amount of GNs (generally with sizes on the order of micrometers edge to edge)[23] was homogenized in an aqueous solution of GOs, followed by sonication. The aqueous dispersion was vigorously stirred, concentrated, and subsequently cast onto a polyvinylidene fluoride (PVDF) surface (GOs forming strong hydrogen bonds with glass surface). The resulting film of about 30 $\mu$m in thickness was peeled off the PVDF surface to be self-standing, followed by further drying in a vacuum oven at ~75 °C. A series of such films of the same total weight but different GN-to-GO ratios were fabricated, so were films of neat GNs and GOs for comparison. The film of neat GNs was rigid and very brittle, but the nanocomposite films were flexible, even at a high loading of GNs (80%, Figure 2).

The films were measured for their in-plane thermal diffusivity ($\kappa$) at room temperature by using the laser-heating angstrom method.[24,25] $\kappa$ is essentially the reduced thermal conductivity ($\lambda$), off by a normalization factor $a$ ($\kappa = \lambda/a$) that accounts for differences in the density $\rho$ and specific heat capacity $C_p$ between different materials, $a = \rho C_p$ (typically close to 2 for nanoscale carbon-based materials). Therefore, $\kappa$ is a more appropriate measure when comparing thermal transport in different materials. As shown in Figure 2, $\kappa$ in the nanocomposites increases monotonically with

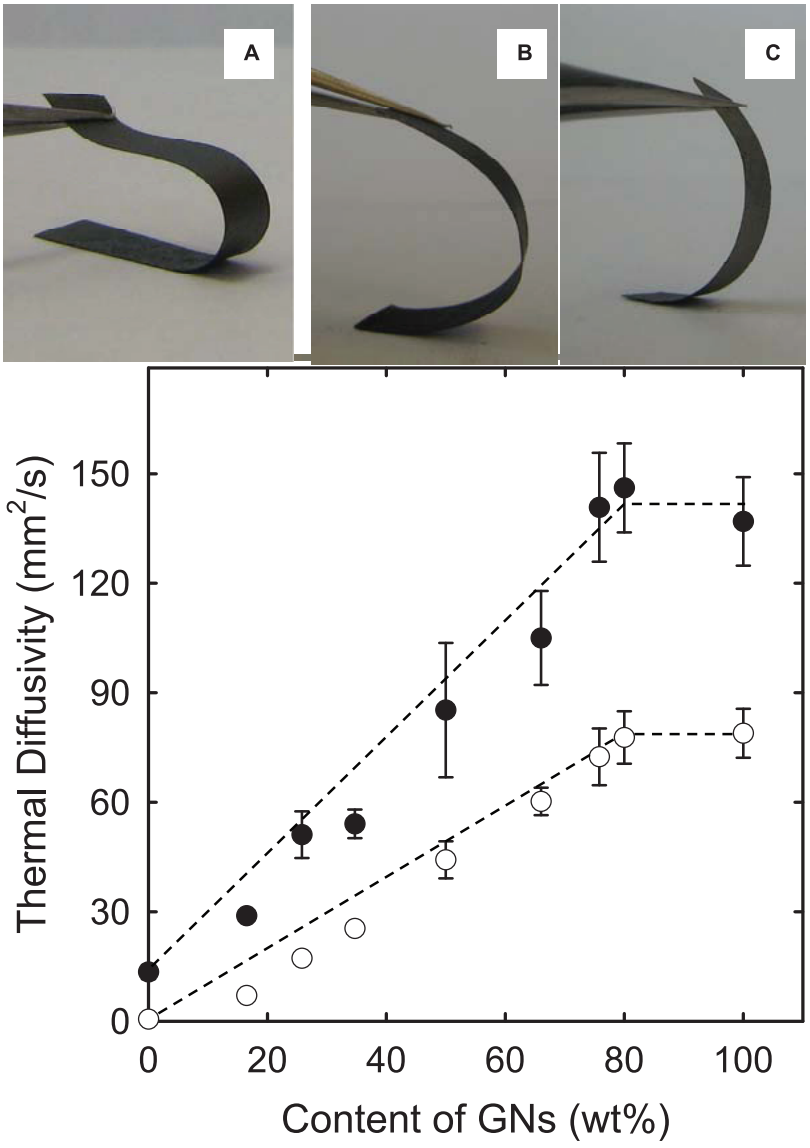


**Figure 2. Top: photos of nanocomposite films containing 50% GNs (A) and 80% GNs (B, as- fabricated; C, after the thermal annealing). Bottom: the observed in-plane thermal diffusivity as a function of the GN loading in the nanocomposite films as fabricated (○) and after the thermal annealing (●), with the error bar denoting standard deviation for multiple data points.**

the increasing content of GNs until reaching a plateau at ~80% loading of GNs ($\kappa \approx 80$ mm$^2$/s). The high $\kappa$ value in the still flexible nanocomposite film (Figure 2) is competitive to those in many highly thermal conductive metals, such as aluminum ($\kappa \approx 84$ mm$^2$/s) and copper ($\kappa \approx 112$ mm$^2$/s). It is also interesting that the thermal transport in the nanocomposite with 80% GNs is at the same level as that in neat film of GNs (Figure 2), despite the thermal insulating nature of GOs as the matrix ($\kappa \approx 0.5$ mm$^2$/s, similar to those found in most polymers). There must be a synergistic effect between GNs and GOs on enhancing thermal transport in these hybrid materials, as the same effect was not observed for nanocomposites of the GNs dispersed in polymeric matrices.[20]

The nanocomposites of GNs dispersed in GOs were characterized by using Raman spectroscopy (632.8 nm excitation). Shown in Figure 3 is a comparison for a typical Raman spectrum of the nanocomposites with those of neat GNs and GOs. The Raman spectra all exhibit G-band (around 1,585 cm$^{-1}$) and broad D-band (around 1340 cm$^{-1}$) features,[22] but the broadness in the G-band and relative intensities between G-band and D-band are different among the three samples. The G-band in neat GOs is very broad, which is apparently carried into the nanocomposite (Figure 3). However, in terms of intensities the spectrum of the nanocomposite is not a superposition of the spectra of its components, as the D-band in the nanocomposite is much too intense relative to the G-band. Besides, GOs are essentially colorless and the GNs have absorption at the excitation wavelength due to extended graphene network, so resonance should have enhanced the Raman signals of GNs in the nanocomposite.

Therefore, the observation of the D-band (intervalley scattering)[26] being more intense suggests an increased amount of defects in the nanocomposite, which might be a result of further exfoliation in the dispersion of the GNs by GOs. The X-ray diffraction pattern for the nanocomposite is more of a superposition of those for GNs and GOs, except for slight peak broadening, again consistent with increased disorder due to further exfoliation and dispersion.

The internal structure of a nanocomposite was probed by using electron microscopy techniques to examine the fracture edges of the nanocomposite film and specimens from cross-sectional microtome. The former were created by stretching the film to failure, and on the edges a representative SEM image is shown in Figure 4, which apparently suggests that the dominating feature in the nanocomposite film is a structure of well-packed layers. The TEM imaging of the specimens from microtome provided a more detailed cross-sectional view of the film structure at the nanoscale. As also shown in Figure 4, the dispersed GNs of various thicknesses are more aligned with the same plane. The thicker pieces (close to 5 nm) are more visible for their higher contrast against the film background and the carbon-coated TEM grid, though the images hardly exclude the presence of other thinner GNs. The electron microscopy results are in general agreement with those found for the nanocomposites of GNs dispersed in conventional polymeric matrices.[20]

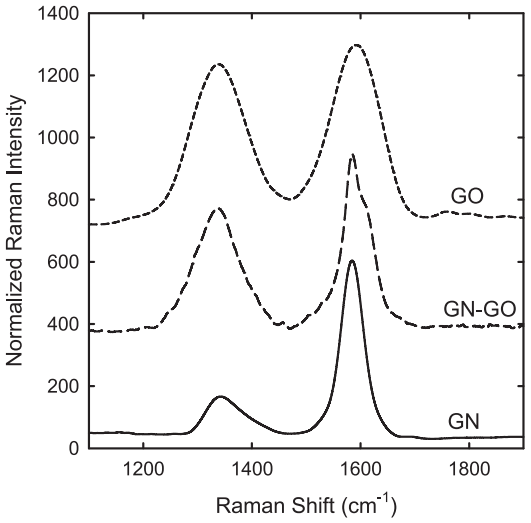


**Figure 3. Raman spectra of a nanocomposite film containing 50% GNs (middle) and films of neat GNs (top) and neat GOs (bottom).**

For the conversion of GOs back to graphene sheets several approaches have been reported in the literature.[6] Among commonly employed methods are chemical reduction with hydrazine and high-temperature heating in an inert environment.[13,28−30] The former has been used for solid-state reduction, where GOs in thin films were exposed to hydrazine vapor, but the conversion has generally been less efficient (than that by the thermal method, for example) to result in a substantial amount of partially reduced byproducts.[28,31] Thus, in this work the neat film of GOs was thermally treated in several steps at different temperatures for the desired conversion while preserving the film structure and morphology. According to thermogravimetric analysis (TGA) of GOs, the majority of the mass loss occurred before 300 °C, producing a significant amount of small gas-phase species (which could potentially cause damages to the film).[15] Therefore, the film of neat GOs was heated in small temperature increments (2 °C/min, in the flow of pure nitrogen gas) to 300 °C, and then a little faster (5 °C/min) to 1100 °C, followed by annealing at 1100 °C for 60 min (still in the flow of pure nitrogen gas). Subsequent measurements of the thermally treated film

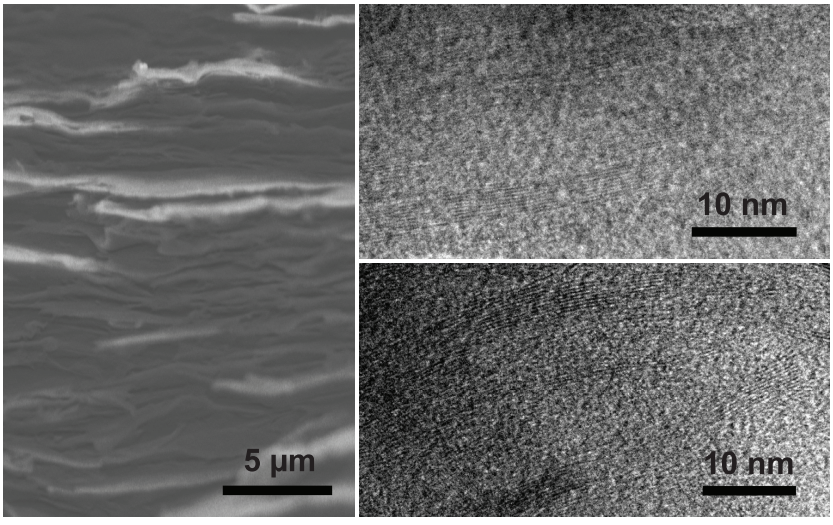


**Figure 4. SEM image on the fracture edge (left) and TEM images on the specimen from cross-sectional microtome (right) of a nanocomposite film containing 50% GNs.**

(neat GOs pretreatment) suggested an improvement in thermal diffusivity by more than an order of magnitude to ~14 $mm^2/s$, though still far lower than the values of GNs and most of their nanocomposites with GOs as fabricated (Figure 2).

The same thermal annealing procedure was applied to the nanocomposites films, also resulting in substantially enhanced thermal transport performance (Figure 2). For example, for the films with 50% and 80% loadings of GNs, the thermal diffusivity values almost doubled to reach 85 $mm^2/s$ and 137 $mm^2/s$, respectively. These are actually higher than those found in the well-known thermal conductive metals such as aluminum and copper. Interestingly, the nanocomposite films after the thermal annealing remained flexible (Figure 2), only slightly less so than pretreatment.

Flexible (plastic-like) thermal conductive nanocomposites have a wide range of potential applications.[32−38] In fact, polymeric (or other soft material-based) nanocomposites of high thermal conductivity are scarce in comparison to those with high electrical conductivity.[38,39] Among nanoscale carbon fillers, carbon nanotubes are well-known for extremely high electrical and thermal conductivities at the individual nanotube level. However, while their dispersion into polymeric matrices beyond percolation does impart substantial electrical conductivity, the enhancement in thermal conductivity is generally much less significant even at very high nanotube loadings due to the nanotube-matrix interfacial barrier toward phonon propagation.[40−42] Various configurations of graphene sheets have been shown as more promising fillers in thermal conductive nanocomposites. For example, Haddon and co-workers processed natural graphite flakes into "graphite nanoplatelets" (GNP) for epoxy nanocomposites of enhanced thermal conductivity (6.44 $W\ m^{-1}\ K^{-1}$ at 25 vol % GNP loading).[32−34] Sun and co-workers dispersed essentially the same fewer-layer GNs used here into polymeric matrices for thermal conductive nanocomposites, with those in epoxy matrices showing the best performance.[20] The dramatically different thermal transport properties between carbon nanotubes and graphene sheets in polymeric/carbon nanocomposites may be rationalized in terms of their different interfacial matches with the matrix for phonon transport,[43] which is dependent on the filler size and shape. In fact, the lateral dimension and thickness of GNs are known to affect significantly the propagation of phonons and the loss associated with boundary scattering.[44−46] The nanocomposites reported here are significantly more thermally conductive than their polymeric counterparts, for which the same rationale may be applied such that interfaces of the filler GNs with the matrix GOs (or restored GOs) are more favorable to phonon transport in the nanocomposites. In addition, microscopically or nanoscopically the GNs and GOs in the nanocomposites are mutually intercalated, which might be more advantageous than the configuration in their polymeric counterparts for thermal diffusion.

## EXPERIMENTAL SECTION

**Materials.** The expanded graphite (surface-enhanced flake graphite, grade 3805) sample was provided by Asbury Carbons. Sulfuric acid (93%), nitric acid (73%), hydrochloric acid (36%), hydrogen peroxide (35%), and phosphorus pentoxide ($P_2O_5$) were obtained from Acros, ammonium persulfate ($(NH_4)_2S_2O_8$) from Aldrich, and postassium permanganate ($KMnO_4$) from Fisher Scientific. PVDF membrane filters (0.2 $\mu$m pore size) were supplied by Fisher Scientific, the dialysis membrane tubing (MWCO ≈ 3500) by Spectrum Laboratories, and carbon-coated copper grids for TEM by SPI Supplies. Water was deionized and purified by being passed through a Labconco WaterPros water purification system.

**GNs.** The as-supplied expanded graphite sample was exfoliated by using a combination of alcohol and oxidative acid treatments.[20] In a typical experiment, the graphite sample (1 g) was added to an alcohol/water mixture (13:7 v/v, 400 mL), stirred at room temperature for 24 h, and then sonicated for another 20 h. The sample was collected *via* filtration and then dried in a vacuum oven. A portion of this sample (500 mg) was added to a nitric acid/sulfuric acid mixture (1:3 v/v, 80 mL) that was precooled in an ice bath. After sonication for 72 h, the mixture was transferred into water (1 L). The GNs were collected *via* filtration, followed by washing repeatedly with deionized water until a neutral pH and drying in a vacuum oven.

**GOs.** The Hummers method[21] with minor modification was used for the preparation of GOs from the same graphite sample. Briefly, concentrated $H_2SO_4$ (10 mL) in a 500 mL flask was heated to 80 °C, to which $(NH_4)_2S_2O_8$ (0.9 g) and $P_2O_5$ (0.9 g) were added. The mixture was stirred until the reagents were completely dissolved. The graphite sample (1 g) was added, and the resulting mixture was heated at 80 °C for 4.5 h. Upon being cooled to room temperature, the reaction mixture was diluted with water (250 mL) and kept for ~12 h. It was then filtrated and washed repeatedly with water, followed by drying in a vacuum oven. The solid sample was added to concentrated $H_2SO_4$ (40 mL) in a 500 mL flask cooled in an ice bath. To the mixture was added slowly $KMnO_4$ (5 g over 40 min), during which the temperature was kept at <10 °C. The reaction mixture, with a change in color from black to greenish brown, was heated at 35 °C for 2 h, followed by dilution with water (85 mL—Caution: the temperature must be kept at <35 °C throughout) and further stirring for 2 h. The reaction mixture was poured into a large beaker, to which water (250 mL) and then aqueous $H_2O_2$ (30%, 10 mL) were added. Bubbles from the aqueous mixture along with a color change to brilliant yellow were observed. After the mixture was allowed to settle for ~12 h, the clear supernatant was decanted, and the sediment was washed repeatedly with aqueous $H_2SO_4$ (5 wt %)−$H_2O_2$ (0.5 wt %) and HCl solution (10 wt %), followed by washing repeatedly with water until no layer separation was observed after centrifuging. The sample was then dialyzed (MWCO ≈ 3500) against water for 7 days to yield a clean aqueous dispersion of GOs. The aqueous GOs thus obtained (acid form) were titrated by aqueous NaOH (0.1 M) until pH 9. The resulting GOs (sodium form) were again dialyzed (MWCO ≈ 3500) for 7 days to reach neutral pH. Finally, the aqueous suspension of GOs was diluted (~0.2 wt %) and sonicated for 30 min to achieve complete exfoliation.

**Nanocomposite Films.** For the fabrication, a weighed amount of GNs (8.3−40 mg) was suspended in an aqueous dispersion of GOs (0.025−0.1 wt %, constant 40 mL) *via* sequential homogenization and sonication for 1 h each. The GN-to-GO ratio was varied, while the total weight was kept constant (50 mg). The suspension was vigorously stirred, concentrated, and subsequently cast onto a polyvinylidene fluoride (PVDF) surface. The film was peeled off to be free-standing, followed by further drying in a vacuum oven at ~75 °C.

**Measurements.** VWR bath sonicator (model 950DA) and homogenizer (Power Gen 125) were used. X-ray powder diffraction measurements were carried out on a Rigaku Ultima IV powder diffraction system. Thermogravimetric analysis (TGA) was performed on a TA Instruments Q500 thermogravimetric analyzer. Raman spectra were obtained on a Johin Yvon T64000 Raman spectrometer equipped with a Melles-Griot He−Ne laser (35 mW) source for 632.8 nm excitation, a triple monochromator, a liquid-nitrogen-cooled symphony detector, and an Olympus BX-41 microscope. Scanning electron microscopy (SEM) images were acquired on Hitachi S4800 FE-SEM system, and transmission electron microscopy (TEM) images on Hitachi HD-2000 S-TEM and Hitachi 9500 TEM systems. For cross-sectional imaging, a film sample was first embedded into epoxy resin and then microtomed into slices less than 100 nm thick by using a Reichert−Jung Ultracut E Microtome with a 308-angle diamond knife at room temperature.

The in-plane thermal diffusivity in the films (typical dimension of 30 mm ×4 mm) was determined by using a commercially acquired ULVAC LaserPIT thermal diffusivity meter (ULVAC Technologies, Inc.)[47] operated in a vacuum of 0.01 Pa at room temperature. The principle behind the instrument is the laser-heating angstrom method.[24,25,47] At least three frequencies were used in the measurement of each film sample, and the readings were averaged for the given specimen.

*Acknowledgment.* This work was made possible by financial support from the Air Force Office of Scientific Research (AFOSR) through the program of Dr. Charles Lee. L.C. was supported by a *Susan G. Komen for the Cure* Postdoctoral Fellowship. C.Y.K. was supported by the Excellent Young Researchers Overseas Visit Program of Japan Society for the Promotion of Science (JSPS). T. J.T. and T.E. were both participants in the Palmetto Academy, an education-training program managed by South Carolina Space Grant Consortium.

## REFERENCES AND NOTES

1. Geim, A. K.; Novoselov, K. S. The Rise of Graphene. *Nat. Mater.* **2007,** *6*, 183–191.
2. Rao, C. N. R.; Sood, A. K.; Subrahmanyam, K. S.; Govindaraj, A. Graphene: The New Two-Dimensional Nanomaterial. *Angew. Chem., Int. Ed.* **2009,** *48*, 7752–7777.
3. Allen, M. J.; Tung, V. C.; Kaner, R. B. Honeycomb Carbon: A Review of Graphene. *Chem. Rev.* **2010,** *110*, 132–145.
4. Zhu, Y.; Murali, S.; Cai, W.; Li, X.; Suk, J. W.; Potts, J. R.; Ruoff, R. S. Graphene and Graphene Oxide: Synthesis, Properties, and Applications. *Adv. Mater.* **2010,** *22*, 3906–3924.
5. Dreyer, D. R.; Ruoff, R. S.; Bielawski, C. W. From Conception to Realization: An Historial Account of Graphene and Some Perspectives for Its Future. *Angew. Chem., Int. Ed.* **2010,** *49*, 9336–9344.
6. Dreyer, D. R.; Park, S.; Bielawski, C. W.; Ruoff, R. S. The Chemistry of Graphene Oxide. *Chem. Soc. Rev.* **2010,** *39*, 228–240.
7. Dikin, D. A.; Stankovich, S.; Zimney, E. J.; Piner, R. D.; Dommett, G. H. B.; Evmenenko, G.; Nguyen, S. T.; Ruoff, R. S. Preparation and Characterization of Graphene Oxide Paper. *Nature* **2007,** *448*, 457–460.
8. Park, S.; Ruoff, R. S. Chemical Methods for the Production of Graphenes. *Nat. Nanotechnol.* **2009,** *4*, 217–224.
9. Boukhvalov, D. W.; Katsnelson, M. I. Modeling of Graphite Oxide. *J. Am. Chem. Soc.* **2008,** *130*, 10697–10701.
10. Erickson, K. E. R.; Lee, Z.; Alem, N.; Gannett, W.; Zettl, A. Determination of the Local Chemical Structure of Graphene Oxide and Reduced Graphene Oxide. *Adv. Mater.* **2010,** *22*, 4467–4472.
11. Li, D.; Muller, M. B.; Gilje, S.; Kaner, R. B.; Wallace, G. G. Processable Aqueous Dispersions of Graphene Nanosheets. *Nat. Nanotechnol.* **2008,** *3*, 101–105.
12. Sun, X. M.; Liu, Z.; Welsher, K.; Robinson, J. T.; Goodwin, A.; Zaric, S.; Dai, H. Nanographene Oxide for Cellular Imaging and Drug Delivery. *Nano Res.* **2008,** *1*, 203–212.
13. Wang, X.; Zhi, L. J.; Mullen, K. Transparent, Conductive Graphene Electrodes for Dye-Sensitized Solar Cells. *Nano Lett.* **2008,** *8*, 323–327.
14. Park, S.; Dikin, D. A.; Nguyen, S. T.; Ruoff, R. S. Graphene Oxide Sheets Chemically Cross-Linked by Polyallylamine. *J. Phys. Chem. C* **2009,** *113*, 15801–15804.
15. Pan, D. Y.; Wang, S.; Zhao, B.; Wu, M. H.; Zhang, H. J.; Wang, Y.; Jiao, Z. Li Storage Properties of Disordered Graphene Nanosheets. *Chem. Mater.* **2009,** *21*, 3136–3142.
16. Wang, L.; Lee, K.; Sun, Y. Y.; Lucking, M.; Chen, Z. F.; Zhao, J. J.; Zhang, S. B. B. Graphene Oxide as an Ideal Substrate for Hydrogen Storage. *ACS Nano* **2009,** *3*, 2995–3000.
17. Kim, J.; Cote, L. J.; Kim, F.; Yuan, W.; Shull, K. R.; Huang, J. X. Graphene Oxide Sheets at Interfaces. *J. Am. Chem. Soc.* **2010,** *132*, 8180–8186.
18. Zhang, C.; Ren, L. L.; Wang, X. Y.; Liu, T. X. Graphene Oxide-Assisted Dispersion of Pristine Multiwalled Carbon Nanotubes in Aqueous Media. *J. Phys. Chem. C* **2010,** *114*, 11435–11440.
19. Tian, L.; Meziani, M. J.; Lu, F.; Kong, C. Y.; Thorne, T. J.; Sun, Y.-P. Graphene Oxide for Homogeneous Dispersion of Carbon Nanotubes. *ACS Appl. Mater. Interfaces* **2010,** *2*, 3217–3222.
20. Veca, L. M.; Meziani, M. J.; Wang, W.; Wang, X.; Lu, F.; Zhang, P.; Lin, Y.; Fee, R.; Connell, J. W.; Sun, Y.-P. Carbon Nanosheets for Polymeric Nanocomposites with High Thermal Conductivity. *Adv. Mater.* **2009,** *21*, 2088–2092.
21. Hummers, W.; Offeman, R. E. Preparation of Graphitic Oxide. *J. Am. Chem. Soc.* **1958,** *80*, 1339.
22. Kudin, K. N.; Ozbas, B.; Schniepp, H. C.; Prud'homme, R. K.; Aksay, I. A.; Car, R. Raman Spectra of Graphite Oxide and Functionalized Graphene Sheets. *Nano Lett.* **2008,** *8*, 36–41.
23. Veca, L. M.; Lu, F.; Meziani, M. J.; Cao, L.; Zhang, P.; Shrestha, M.; Sun, Y.-P. Polymer Functionalization and Solubilization of Carbon Nanosheets. *Chem. Commun.* **2009,** 2565–2567.
24. Hakovirta, M.; Vuorinen, J. E.; He, X. M.; Nastasi, M.; Schwarz, R. B. Heat Capacity of Hydrogenated Diamond-like Carbon Films. *Appl. Phys. Lett.* **2000,** *77*, 2340–2342.
25. Takahashi, F.; Fujii, K.; Hamada, Y.; Hatta, I. Thermal Diffusivity Measurement of Chemical-Vapor-Deposited Diamond by an AC Calorimetric Method. *Jpn. J. Appl. Phys. Part 1: Regul. Pap. Short Notes Rev. Pap.* **2000,** *39*, 6471–6473.
26. Sato, K.; Saito, R.; Oyama, Y.; Jiang, J.; Cancado, L. G.; Pimenta, M. A.; Jorio, A.; Samsonidze, G. G.; Dresselhaus, G.; Dresselhaus, M. S. D-Band Raman Intensity of Graphitic Materials as a Function of Laser Energy and Crystallite Size. *Chem. Phys. Lett.* **2006,** *427*, 117–121.
27. Pimenta, M. A.; Dresselhaus, G.; Dresselhaus, M. S.; Cancado, L. G.; Jorio, A.; Saito, R. Studying Disorder in Graphite-Based Systems by Raman Spectroscopy. *Phys. Chem. Chem. Phys.* **2007,** *9*, 1276–1291.
28. Becerril, H. A.; Mao, J.; Liu, Z.; Stoltenberg, R. M.; Bao, Z.; Chen, Y. Evaluation of Solution-Processed Reduced Graphene Oxide Films as Transparent Conductors. *ACS Nano* **2008,** *2*, 463–470.
29. Lomeda, J. R.; Doyle, C. D.; Kosynkin, D. V.; Hwang, W. F.; Tour, J. M. Diazonium Functionalization of Surfactant-Wrapped Chemically Converted Graphene Sheets. *J. Am. Chem. Soc.* **2008,** *130*, 16201–16206.
30. Tung, V. C.; Allen, M. J.; Yang, Y.; Kaner, R. B. High-Throughput Solution Processing of Large-Scale Graphene. *Nat. Nanotechnol.* **2009,** *4*, 25–29.
31. Yang, D.; Velamakanni, A.; Bozoklu, G.; Park, S.; Stoller, M.; Piner, R. D.; Stankovich, S.; Jung, I.; Field, D. A.; Ventrice, C. A..;; *et al*.Chemical Analysis of Graphene Oxide Films after Heat and Chemical Treatments by X-ray Photoelectron and Micro-Raman Spectroscopy. *Carbon* **2009,** *47*, 145–152.

32. Yu, A. P.; Ramesh, P.; Itkis, M. E.; Bekyarova, E.; Haddon, R. C. Graphite Nanoplatelet−Epoxy Composite Thermal Interface Materials. *J. Phys. Chem. C* **2007,** *111*, 7565–7569.
33. Yu, A. P.; Ramesh, P.; Sun, X. B.; Bekyarova, E.; Itkis, M. E.; Haddon, R. C. Thermal Conductivity in a Hybrid Graphite Nanoplatelet—Carbon Nanotube Filler for Epoxy Composites. *Adv. Mater.* **2008,** *20*, 4740–4744.
34. Sun, X.; Ramesh, P.; Itkis, M. E.; Bekyarova, E.; Haddon, R. C. Dependence of the Thermal Conductivity of Two-Dimensional Graphite Nanoplatelet-Based Composites on the Nanoparticle Size Distribution. *J. Phys.: Condens. Matter* **2010,** *22*, 334216.
35. Kalaitzidou, K.; Fukushima, H.; Drzal, L. T. Multifunctional Polypropylene Composites Produced by Incorporation of Exfoliated Graphite Nanoplatelets. *Carbon* **2007,** *45*, 1446–1452.
36. Ghose, S.; Watson, K. A.; Working, D. C.; Connell, J. W.; Smith, J. G.; Sun, Y.-P. Thermal Conductivity of Ethylene Vinyl Acetate Copolymer/Nanofiller Blends. *Compos. Sci. Technol.* **2008,** *68*, 1843–1853.
37. Ghosh, S.; Calizo, I.; Teweldebrhan, D.; Pokatilov, E. P.; Nika, D. L.; Balandin, A. A.; Bao, W.; Miao, F.; Lau, C. N. Extremely High Thermal Conductivity of Graphene: Prospects for Thermal Management Applications in Nanoelectronic Circuits. *Appl. Phys. Lett.* **2008,** *92*, 151911.
38. Kuillar, T.; Bhadra, S.; Yao, D.; Kim, N. H.; Bose, S.; Lee, J. H. Recent Advances in Graphene Based Polymer Composites. *Prog. Polym. Sci.* **2010,** *35*, 1350–1375.
39. Moniruzzaman, M.; Winey, K. I. Polymer Nanocomposites Containing Carbon Nanotubes. *Macromolecules* **2006,** *39*, 5194–5205.
40. Nan, C. W.; Shi, Z.; Lin, Y. A Simple Model for Thermal Conductivity of Carbon Nanotube-Based Composites. *Chem. Phys. Lett.* **2003,** *375*, 666–669.
41. Shenogin, S.; Xue, L. P.; Ozisik, R.; Keblinski, P.; Cahill, D. G. Role of Thermal Boundary Resistance on The Heat Flow in Carbon-Nanotube Composites. *J. Appl. Phys.* **2004,** *95*, 8136–8144.
42. Shenogina, N.; Shenogin, S.; Xue, L.; Keblinski, P. On The Lack of Thermal Percolation in Carbon Nanotube Composites. *Appl. Phys. Lett.* **2005,** *87*, 133106–133113.
43. Lin, W.; Zhang, R. W.; Wong, C. P. Modeling of Thermal Conductivity of Graphite Nanosheet Composites. *J. Electron. Mater.* **2010,** *39*, 268–272.
44. Ghosh, S.; Bao, W.; Nika, D. L.; Subrina, S.; Pokatilov, E. P.; Lau, C. N.; Balandin., A. A. Dimensional Crossover of Thermal Transport in Few-layer Graphene. *Nat. Mater.* **2010,** *9*, 555–558.
45. Nika, D. L.; Pokatilov, E. P.; Askerov, A. S.; Balandin, A. A. Phonon Thermal Conduction in Graphene: Role of Umklapp and Edge Roughness Scattering. *Phys. Rev B* **2009,** *79*, 155413.
46. Xiang., J.; Drzal, L. T. Thermal Conductivity of Exfoliated Graphite Nanoplatelet Paper. *Carbon* **2011,** *49*, 773–778.
47. http://www.ulvac.com/thermal/laserpit.asp (last accessed March 2011).